SUPPLEMENTAL (SUPPORTING) DATA

Purification and Expansion of BM-Derived Mouse Bone Marrow Progenitor Cells (mBMPCs)

Purification and expansion of BM-derived mBMPCs entails the use of ECM matrix coated dishes and EBM-2 media supplemented with specific growth factors. As depicted in Figure S1A, an adherent sub-population of cells (hereafter referred to as passage 1 (p1) mBMPCs) appeared as early as 6-7 days. P1 cells were expanded up to p5 and their morphology was examined using light microscopy, Figure S1B-E. We have termed p2 and p3 cells (equivalent to 2 population doublings) as early-growth mBMPCs (21-22 days in culture). These cells are 60-70% adherent morphology. However, by p4 (23-24 days in culture), mBMPCs became more homogeneous morphology Figure S1D, and mBMPCs that were cultured up to p5 (26-27 days in culture) displayed an elongated structure, Figure S1E. To minimize cell culture induced artifacts, all experiments were performed using p3 mBMPCs. Next, we performed Western blot analysis to determine the expression of known endothelial cell antigens. As shown in Figure S1F, the expression of Flk1 in mouse lung endothelial cells (mEC_3, passage3) was minimal. Interestingly, p1 to p3 mBMPCs showed a steady increase in Flk1 expression, while the expression of Flk1 was robust at p4 and p5, Figure S1F. Expression of VE-cadherin was low at p1 to p3, but appeared to increase steadily with increasing passage, however, the expression of VE-cadherin at p3-p5 were about 50-60% lower than that of mature mECp3 (first lane), Figure S1G. We observed a similar pattern of expression for β_1 and caveolin-1, Figure S1G-I. We also detected low level expression of Tie-2 and Lipid phosphate phosphatase-3 (Lpp3), Figure S1J-K. We did not detect change in the expression of adapter protein Grb2 (control), Figure S1L.

Adhesion of mBMPCs onto Purified ECM Proteins and Formation of Focal Adhesion Sites and Tyrosine Phosphorylation of Fak

We performed a cell adhesion assay to examine the ability of mBMPCs integrins to bind specific ECM molecules by preparing increasing concentrations of fibronectin (Fn), vitronectin (Vn), laminin-1 (Lm-1), and laminin-4 (Lm-4). Pilot experiments were performed to determine the optimal concentration of ECM components required for mBMPCs adhesion. Heat-inactivated BSA was included as a negative control and used to block ECM pre-coated dishes. Binding of mBMPCs to heat-inactivated BSA was minimal and considered baseline. As shown in Figure S2A, at lower concentrations (12.5, 25, and 50 nM) we observed a concentration-dependent adhesion of mBMPCs to Lm-1, Lm-4, Fn, and Vn. In contrast, higher concentrations of ECM (75 and 100 nM) did not promote a further increase in mBMPCs adhesion. Addition of EDTA (1 and 2 mM) blocked integrin mediated cell adhesion, indicating that mBMPCs attachment required the presence of Ca^{2+} and Mg^{2+}. Representative images of cell adhesion are shown in Figure S2B and D. Interestingly, mEPCs plated on Fn and Vn were spread compared to those plated on Lm-1 or Lm-4.

We next determined whether adhesion of mBMPCs to fibronectin induces the formation of focal adhesion sites (ECM cell junctions), tyrosine phosphorylation of Fak, and Erk1/2 activation. Indeed, we observed that adhesion of mouse lung endothelial cells (mEC) (positive control) and mBMPCs onto fibronectin induced formation of focal adhesion sites, Figure S2F and G (indicated by white arrows). Focal adhesion site formation was associated with a highly organized cytoskeleton with actin containing microfilaments and fiber-like structures (Figure S2F, G). The observation that adhesion of mBMPCs formed focal adhesion sites on fibronectin points to the involvement of intracellular signaling. To pursue this question, we examined the possibility that adhesion of mBMPCs to fibronectin

leads to changes in tyrosine phosphorylation of Fak. As shown in Figure S2H, we observed tyrosine phosphorylation of Fak in mBMPCs in response to adhesion onto Lm-1, Lm-4, Fn, and Vn, whereas BSA failed to do so. In addition, we observed Erk1/2 phosphorylation (Figure S2J). Thus, mBMPCs integrins are adhesion-competent and $\alpha_4\beta_1$ and $\alpha_5\beta_1$ integrins are functional on fibronectin and induce formation of focal adhesion sites and induce tyrosine phosphorylation of Fak.

Effects of Irradiation

Because γ-irradiation used (see *Methods*) causes neutropenia, we first determined PMN uptake in mouse lungs after LPS challenge with and without the irradiation step. Based on preliminary studies, a combination of irradiation (5 Gy) and LPS (7.5 mg/kg BW) was chosen to yield 50% mortality at 12 hr with the remaining dying after another 12 hr (data not shown). Lung MPO activity was used as a surrogate marker of lung PMN sequestration (Figure S5A). MPO activity increased 3-fold at 4 hr in the C57BL control mice, peaked at 6 hr, declined at 12 hr, and then returned to baseline at 24 hr (Figure S5B). At 6 hr, LPS alone increased MPO activity, whereas γ-irradiation + LPS resulted in smaller increase in MPO activity. At 12 and 24 hr, MPO activities of the two groups decreased similarly, and after 24 hr, the MPO activities in both groups were comparable to the 4 hr values**.** Histological of lungs showed no change in lung architecture in control and irradiated mice 24 hr after challenge (Figure S5C, D). In contrast, lungs of LPS alone or irradiated plus LPS-injected mouse lungs showed alveolar wall thickening, interstitial and alveolar hemorrhage, and influx of PMNs and monocytes (Figure S5E, F). Thus, γ-irradiation did not significantly alter PMN sequestration in lungs in response to LPS injury.

SUPPLEMENTAL METHODS

Cell Adhesion Assay on Purified ECM Molecules

Lm-1, Lm-4, Fn, and Vn were prepared at concentrations of 12.5, 25, 50, 75, and 100 nM in Tris-buffered saline (20 mM Tris, pH.7.4 and 150 mM NaCl) as previously described [27, 29], and heat inactivated 0.2% bovine serum albumin (BSA) was included as control. Sterile 24 micro wells were coated overnight at 4 °C with increasing concentrations of the above substrates. EPCs were pre-treated with monensin and cycloheximide for 1 hr, cells were detached with 3 mM EDTA, pH 7.4, washed with PBS, and passed through a cell strainer to remove unwanted cell aggregates. The cells were collected and resuspended in EGM-2, 0.2% BSA, and 1x insulin/transferrin/selenium-A supplemented with 1 mM Mg^{2+} and Ca^{2+}. To the well, 100 µl of cell suspension (0.5×10^5 cells/ml) was added and allowed to attach at 37°C in a humidified CO_2 incubator for indicated times. Fixing, staining, elution, and cell adhesion assays were performed as previously described [27, 29]. For focal adhesion staining, cells were seeded onto glass coverslips pre-coated with fibronectin (5.0 µg/ml), allowed to attach for 120 minutes, and fixed. Fixed cells were stained with anti-vinculin mAbs and TRITC-phalloidin, and analyzed by fluorescent microscopy as previously described [27].

Cell Migration and Scratch Assays

A modified Boyden chamber was used to measure haptotactic and chemotactic migration. ECM molecules, $VEGF^{165}$, and cell suspensions were prepared in EBM-2 containing 0.2% heat inactivated BSA. Briefly, a polycarbonate filter with 12-µm pores (Corning Costar, Corning, NY) was coated with ECM molecules (5 µg/ml), and experiments were performed using triplicate polycarbonate filters for each time point. Filters were placed on a 24-well chamber (Corning Costar) containing 400 µl of $VEGF^{165}$ (50 ng/ml), mECs, and mBMPCs (5,000 cells in 200 µl/well) were loaded into the upper compartment, and isotype matched IgG and anti-VEGF monoclonal antibodies (50 µg/ml) were added to the lower chamber. After incubation at 37°C in 5% CO_2 for 6 hrs, the filter was disassembled, the cells on the filter were fixed with 3.7% PFA, and stained with a 0.5% crystal violet. Non-migratory cells from the upper face of the filter were removed by q-tip. The cells that migrated to the lower face of the membrane were counted using a light microscope at 200X. At least 6 random fields were chosen for each filter, and experiments were performed at least 3 times. Data were calculated as a percent cell migration, for example: on vitronectin + VEGF+ IgG, out of ~5,000 cells plated onto the upper chamber, only ~750 cells migrated to the lower face of the filter. This data was calculated as 15.56 ± 3.57 % (n=12) cell migration. For scratch assay, mBMPCs were plated at high density (10^7 cells/ml) on glass coverslips, grown for 3 days in order to reach a confluent monolayer, and a white pipette tip (10 µl tip) was used to draw several scratch lines on to the monolayer. Cells that came off the glass coverslips were washed off with PBS, and remaining cells were provided with EBM-2 media supplemented with $VEGF^{165}$ (50 ng/ml). Cells were incubated at $37^{O}C$, and wound closure was monitored at 0, 4, and 8 hrs.

Western Analysis

For tyrosine phosphorylation, cells were detached with 3 mM EDTA (pH 7.4), washed with PBS, maintained in suspension for 45 min at room temperature, and then replated onto dishes coated with the indicated substrates at 37 °C in a CO_2 incubator. After 30 or 45 minutes, cells were solubilized in cell extraction buffer (50 mM HEPES, pH 7.5; 150 mM NaCl; 1% Triton X-100; 25 mM sodium fluoride; 2 mM sodium orthovanadate; 1 mM sodium

pyrophosphate; and protease inhibitors). Preparation of cell extracts, protein quantification, and Western analysis have been previously described [27-29].

Fluorescent Activated Cell Sorting (FACS)

Because of limited number of cells at passage-1 (p1) and p2, FACS analysis for integrin expression was not determined until p3. The p3 mBMPCs were washed in PBS (pH 7.4), detached with 0.025% trypsin and 3 mM EDTA in PBS (pH 7.4), washed once in PBS containing Ca^{2+} and Mg^{2+}, and then passed through a cell strainer. The cells (1×10^6) were then incubated with saturating amounts of control mouse IgG or the following anti-mouse (or rat) monoclonal antibodies (Table I). These methods have been described in detail elsewhere [31-33].

^{35}S-Cys/Met Labeling of EPCs and Tissue Distribution

Radioactive labeling of cells was performed as previously described [29]. Briefly, mBMPCs (5×10^7) were grown in Cys/Met-free growth DMEM for 8 hours. Cells were then incubated with 2 mCi of ^{35}S-Cys/Met (specific activity 1170.0 Ci/mmol) for 2 hours at 37 °C in Cys/Met-free DMEM in the presence of 1 X ITS. Media containing radioactive ^{35}S-Cys/Met was removed, and cells were rinsed twice with complete media and allowed to recover in complete media for 1 h at 37 °C. Cells were then detached with 3.5 mM EDTA (pH 7.4), washed with PBS, and passed through an 80-μM sterile cell strainer. Number of cells was determined. EPCs were resuspended in sterile PBS at a concentration of 400,000 EPCs/100 μl. Total radioactive counts of 2.5×10^7 CPM/400,000 mBMPCs were adjusted to 100%. mBMPCs were then administered as described above.

Differentiation Potential of mEPCs

The bFGF- and VEGF-induced branching point structure as a measure of morphogenic differentiation of mBMPCs in three-dimensional type I collagen matrix was performed as previously described with minor modifications [27, 28]. Briefly, mBMPCs were detached from dishes with 3 mM EDTA, washed with PBS, suspended in defined medium (EBM-2 medium containing 5% FBS, 1X insulin, transferrin, and selenium [ITS]), and seeded onto a collagen matrix. Approximately 0.1×10^6 mBMPCs were incubated with 50 μg/ml of control IgG, anti-α_1, anti-α_2, anti-α_3, anti-α_4, anti-α_5, anti-α_6, or anti-$\alpha_v\beta_3$ integrin mAbs on ice for 45 min. The mBMPCs were then washed and resuspended in defined medium. The cells were then cultured with FGF-2 (20 ng/ml) and VEGF (50 ng/ml) for 16 hrs in a humidified CO_2 incubator at 37 °C. Cells were fixed with 4% PFA and washed with PBS. Photographs were taken under a phase-contrast microscope. For quantification of branching points, at least 10 random fields were chosen. Experiments were repeated 3 times.

Statistical Analysis

GraphPad Prizm software was used for most statistical analyses. We used Student's unpaired two-tailed *t*-test for most analyses. Comparisons between experimental groups were made by ANOVA with a significance value set at $p<0.05$. For the survival study, we used the Kaplan-Meier and log-rank tests.

Supplementary Figure legends:

Figure S1. Morphology of cultured mBMPCs. **A**) A single colony outgrowth of mBMPCs (p1) at 6-7 days in culture. (**B**-**E**) mBMPCs at p2-p5 were fixed and stained with Eosin. (**F**-**L**) mEC3 (control, mouse lung endothelial cells extract at p3) and mBMPCs total lysates were subjected to western blot (WB) analysis with indicated antibodies. Data are representative of at least three independent experiments.

Figure S2. Characterization of mouse mBMPCs. mECs or mBMPCs (4×10^5) were incubated with **A**-**I**) control IgG, anti-α_1, anti-α_2, anti-α_3, anti-α_4, anti-α_5, anti-α_6, anti-α_v, or anti-β_1 mAbs and **J**-**L**) Anti-CD34, anti-VE-cadherin and anti-Flk-1 mAbs were included as control markers for mBMPCs and mEC, respectively. Antibody binding was detected after incubation with FITC-conjugated goat anti–rat/hamster IgG. Data are representative of at least three independent experiments.

Figure S3. Adhesion of mECs and mBMPCs on purified substrates; and mBMPCs adhesion events are mediated by $\alpha_4\beta_1$ and $\alpha_5\beta_1$ integrins. **A**) Dishes were coated either with BSA (0.2%) or with increasing concentrations (12.5, 25, 50, 75, and 100 nM) of indicated ECM substrates and static cell adhesion assays were performed as described in Methods. Data presented as mean ± SD, n=15. **B** - **E**) Morphology of attached mEPCs on indicated ECM molecules. Magnification, 200×. Scale bar, 150 μm. Data are representative of at least three independent experiments. Formation of focal adhesion sites in mouse lung endothelial cells (mECs) **F**) and mBMPCs **G**) was detected by immunostaining with anti-vinculin mAb (green) and TRITC-phalloidin (red); DAPI (blue). Magnification 400×, bar = 150 μm. **H**) Adhesion of induced Fak phosphorylation were analyzed by immunoblotting with anti-p-Fak (397Y) pAb. (**I**) To ensure equal loading of proteins, membrane was stripped and reprobed with anti-Fak mAb. Phosphorylated Erk 1/2 and Erk 1/2 expression are indicated in **J** and **K**. Data are representative of at least three independent experiments.

Figure S4. Indirect immunofluorescence microscopy analysis of expression of vWF by mBMPCs. **A**-**P**) Control mECs and mBMPCs grown on gelatinized coverslips were stained with indicated control rabbit IgG or rabbit anti-vWF polyclonal antibodies. F-actin was visualized with TRITC-phalloidin. Scale bars indicate 50 μm. Images are representative of at least three independent experiments. **Q**-**S**) Total cell lysate prepared from mEC (C) and mBMPCs at 1 to 5 passages were subjected to western blotting analysis with indicated antibodies. Note that control mEC express mature vWF (~220 kDa), while mBMPCs express slow moving immature vWF polypeptide (~220-350 kDa) species. Data are representative of at least three independent experiments.

Figure S5. Lung MPO activity and kinetics of distribution of ^{35}S-Met/Cys-labeled EPCs. **A**) Experimental time-line schematic for MPO assay. **B**) Lungs were removed and weighed; right lung was used for MPO assay and left lung for sectioning and histology. Equal amount of protein was used for MPO activity. Untreated and irradiated mice showed equal MPO activity/gm tissue, and their values were adjusted to baseline. Data represent mean ± SEM from 5 animals. $*p < 0{\cdot}01$ *vs.* γ-radiation + LPS at 0 h, $**p < 0{\cdot}001$ *vs.* γ-radiation + LPS at 0 h. **C**-**F**) H&E-stained sections. Magnification 100X. Scale bar, 150 μm.

Figure S6. Representative confocal images of retention and engraftment of mBMPCs at the end of 8 weeks. **A, C)** Lung sections were stained with anti-RFP-antibody (green), CD34

(red); (**B, D**) stained with anti-RFP antibody (green) and anti-Flk1 (pacific blue, yellow arrows) analyzed by confocal microscopy. At the end of 8 weeks the intensity of CD34 (red) and Flk1 (pacific blue, yellow arrows) were very low. Magnifications are as shown. Data are representative of at least three independent experiments.

Figure S7. Quantification of retention of mBMPCs expressing RFP examined at the end of 48 hrs by staining with an anti-RFP polyclonal antibody (see Figure 4L-O). The number of RFP-positive mBMPCs per 200X field is shown. Data are representative of at least three independent experiments. * $p< 0.02$ *vs.* γ + LPS + EPC group.

Figure S8. Effect of mBMPCs administration in LPS-injured nude mice. **A**) Survival analysis among nude athymic mice that were treated with PBS (n=18, control PBS) or treated with LPS (22.5 mg/kg BW) i.p. (n=24, LPS control), or mice receiving mBMPCs ($4X10^5$/animal r.o.) 4 hours after LPS treatment (n=24, LPS + mBMPCs). At 48 hours, mBMPCs treatment significantly increased survival compared with LPS control (60% *vs*. 45%, $p <0.05$). At 96 hours, mBMPCs increased survival compared with LPS control (60% *vs*. 15%, $p <0.01$). **B)** Lung water content (wet *vs* dry) in nude athymic mice 12 hours (i.e., 8 hr after mBMPCs treatment) after LPS treatment (n=18 each group). At 12 hours, there was significant reduction in lung water content in mice receiving mBMPCs (8.11 $\pm$ 0.476 *vs* 5.22 $\pm$ 0.356). LPS = lipopolysaccharide; i.p. intraperitoneal; r.o., retro=orbital.

Figure S9. Indirect immunofluorescence microscopy of mBMPCs sequestration. **A-D**) Intercalation of mBMPCs with resident endothelial cell was a rare event. At the end of 96 hours, a single RFP-expressing mBMPCs (red) colocalized within vWF positive vascular structure (green) in the lung. **E-H**) While, confocal microscopy analysis showed that RFP-expressing mBMPCs (red) did not colocalize with macrophage F4/80 (green). Photomicrographs were taken using a 40X objective. The results are representative of those obtained from three independent experiments. Scale bar, 100 μm.

Figure S1 (Wary et al, 2009)

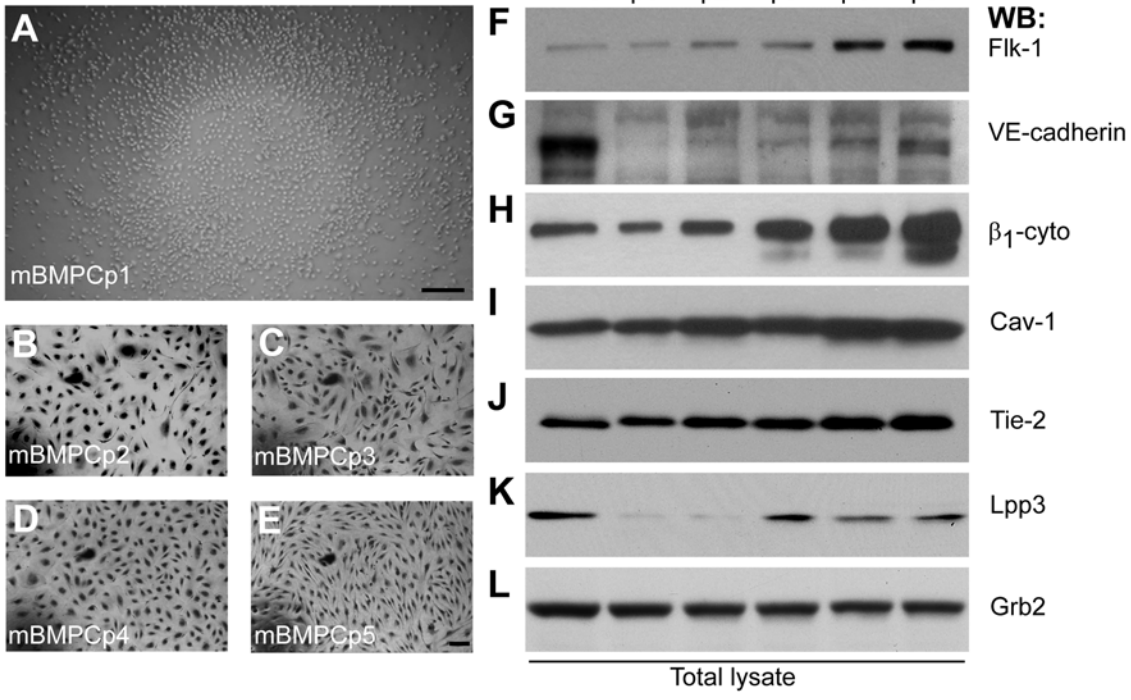

Figure S2 (Wary et al, 2009)

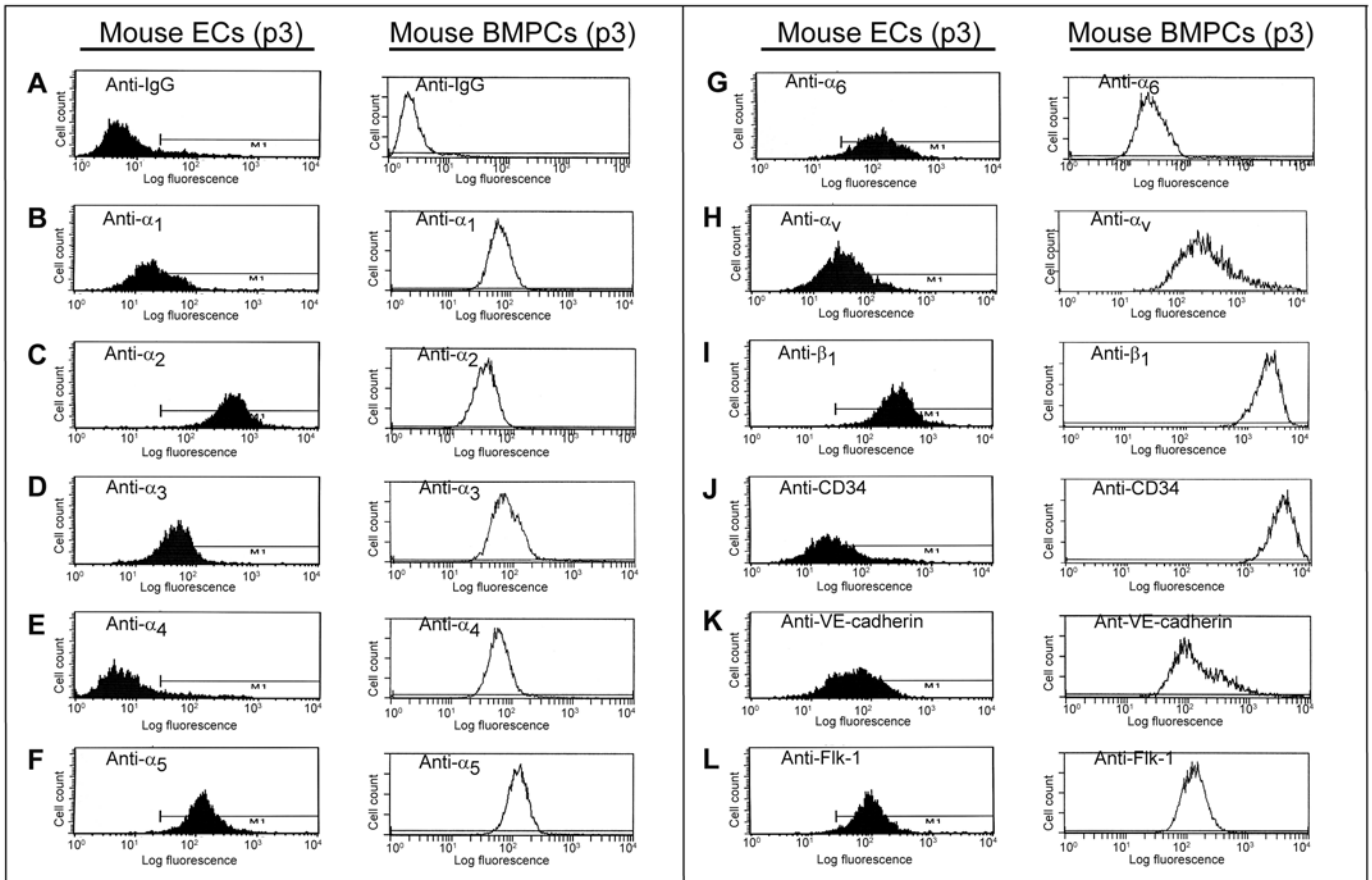

Figure S3 (Wary et al, 2009)

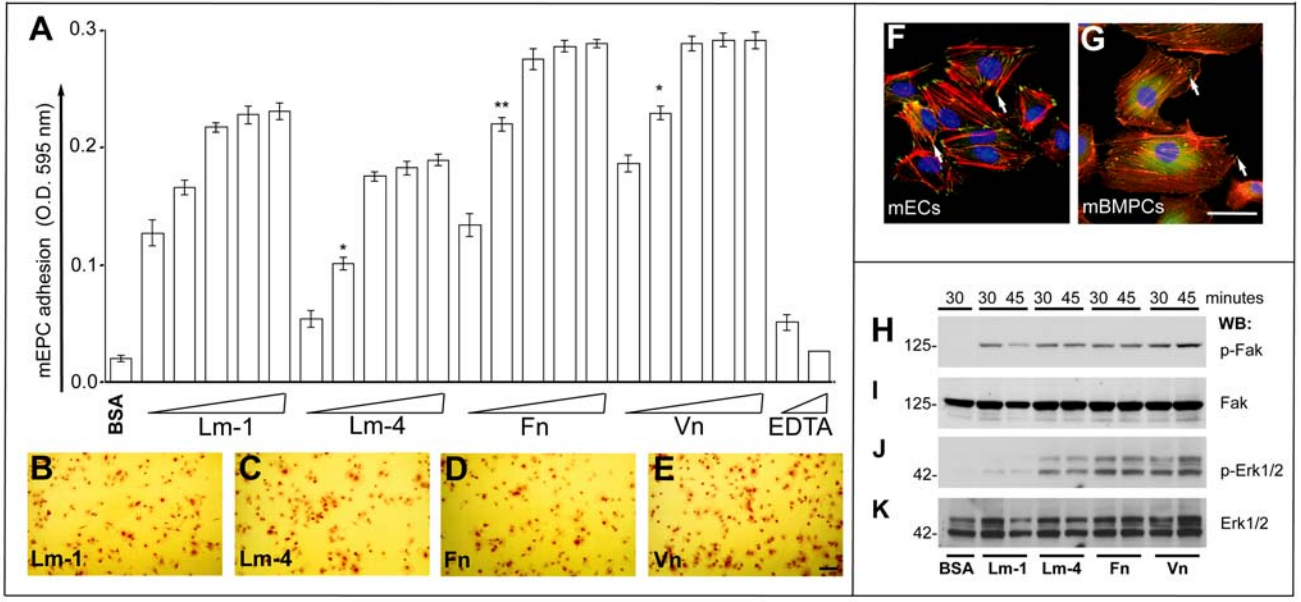

Figure S4 (Wary et al, 2009)

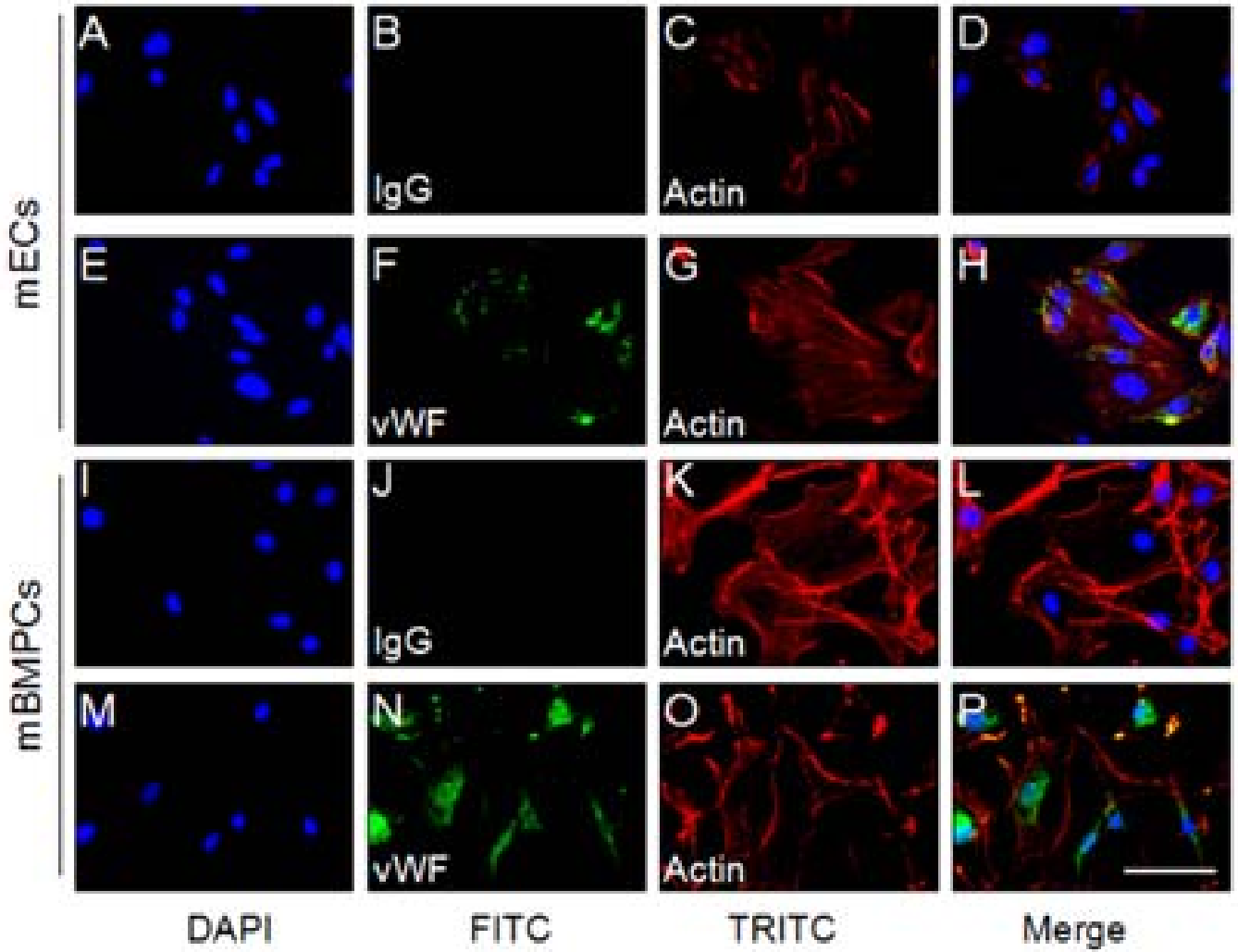

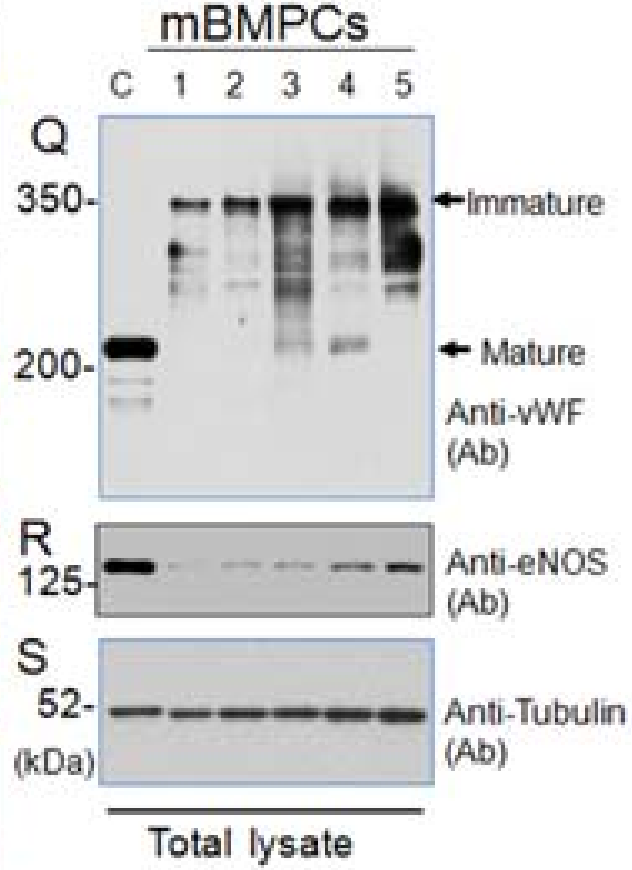

Figure S5 (Wary et al, 2009)

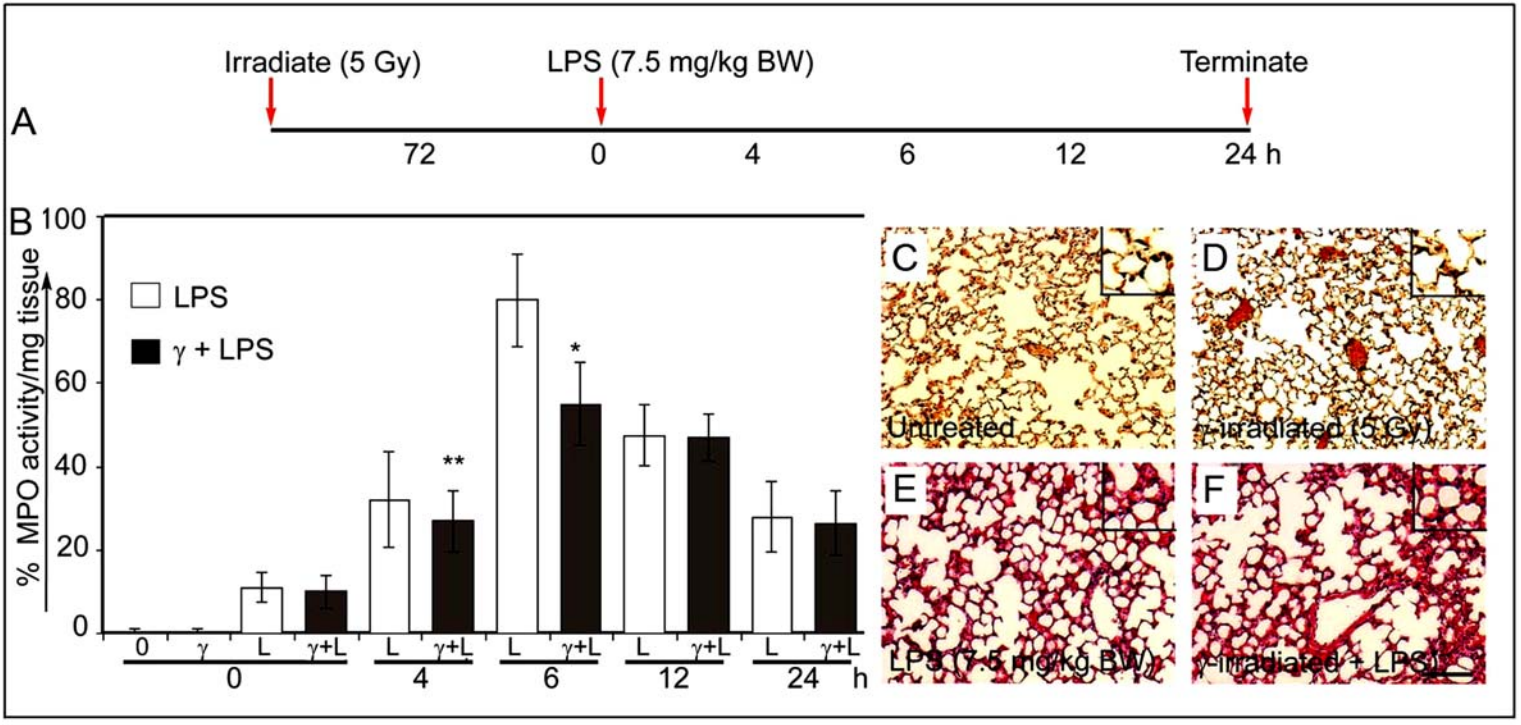

Figure S6 (Wary et al, 2009)

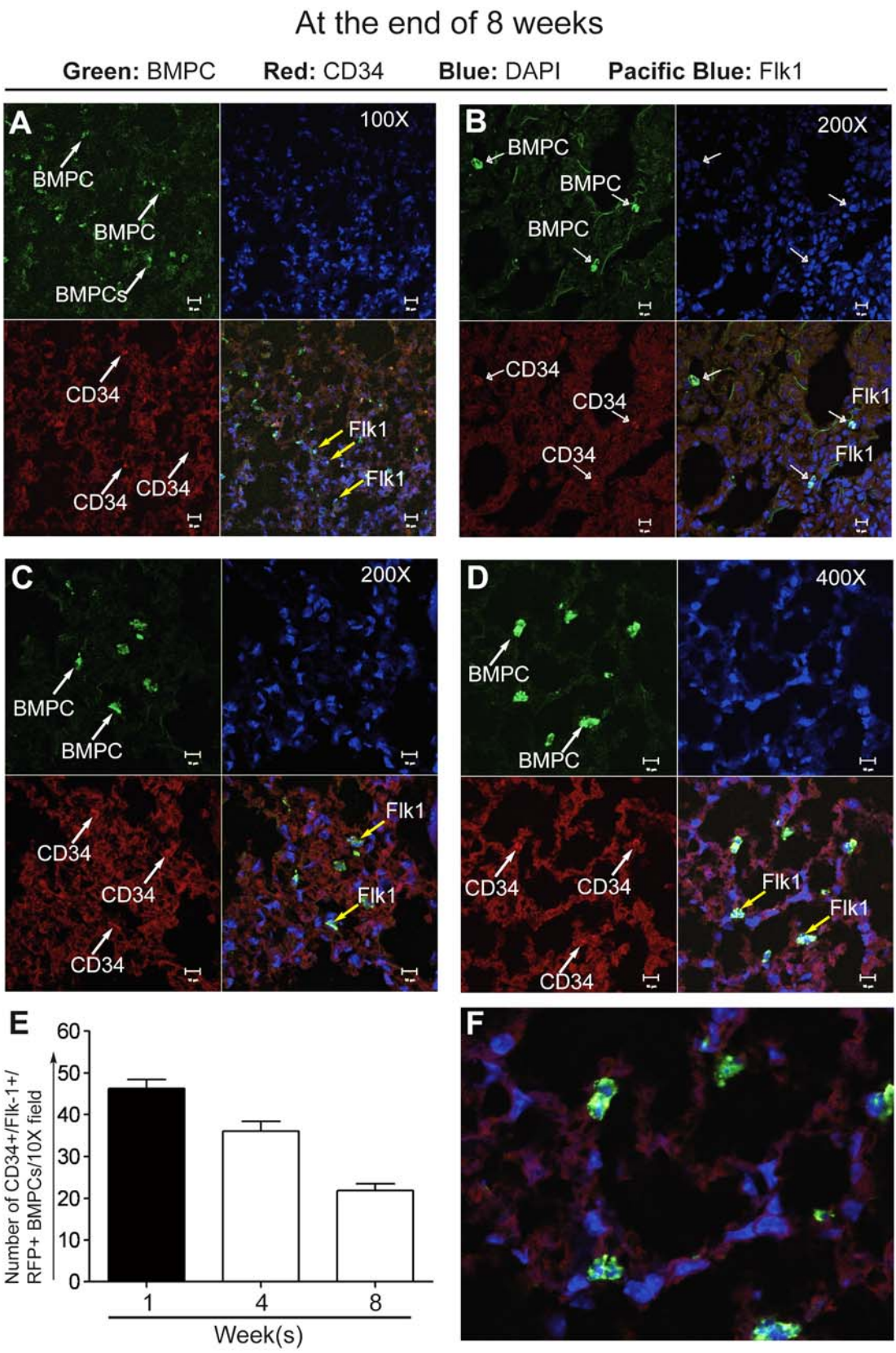

Figure S7 (Wary et al, 2009)

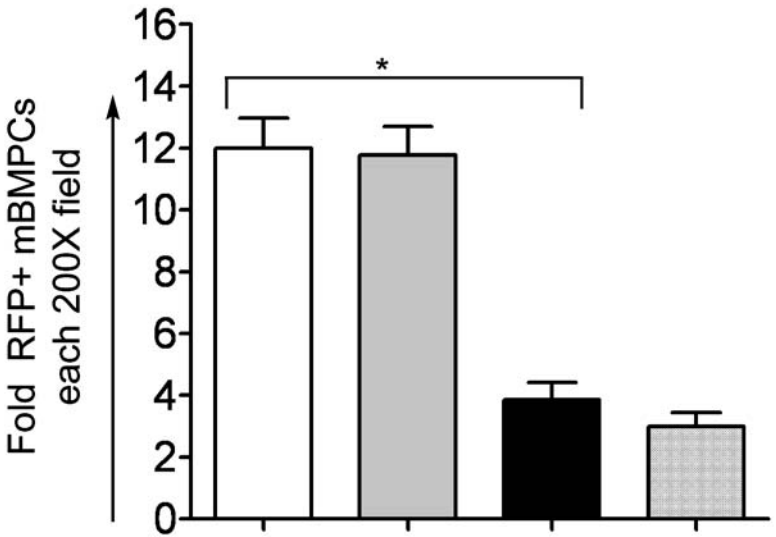

γ-irradiation	+	+	+	+
LPS	+	+	+	+
α_2-shRNA	-	+	-	-
α_4-shRNA	-	-	-	+
α_5-shRNA	-	-	+	-

Figure S8 (Wary et al, 2009)

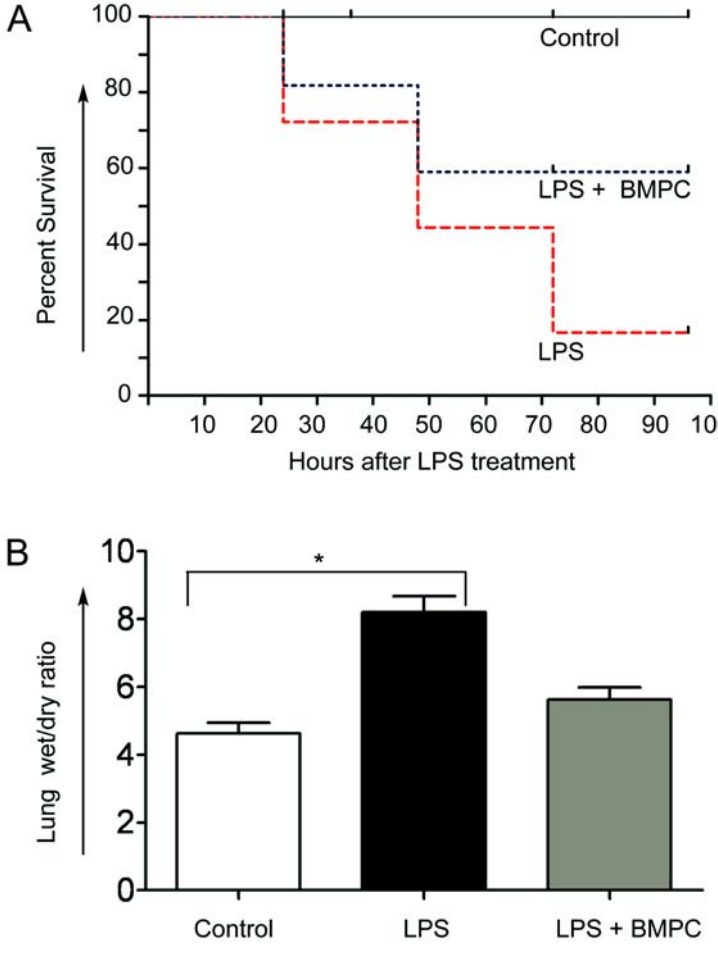

Figure S9 (Wary et al, 2009)